

^{11}Li Breakup on ^{208}Pb at Energies Around the Coulomb Barrier

J. P. Fernández-García,^{1,2} M. Cubero,^{3,4} M. Rodríguez-Gallardo,¹ L. Acosta,^{5,6} M. Alcorta,³ M. A. G. Alvarez,^{1,2} M. J. G. Borge,³ L. Buchmann,⁷ C. A. Diget,⁸ H. A. Falou,⁹ B. R. Fulton,⁸ H. O. U. Fynbo,¹⁰ D. Galaviz,¹¹ J. Gómez-Camacho,^{1,2} R. Kanungo,⁹ J. A. Lay,¹ M. Madurga,³ I. Martel,¹² A. M. Moro,¹ I. Mukha,¹ T. Nilsson,¹³ A. M. Sánchez-Benítez,¹² A. Shotter,¹⁴ O. Tengblad,³ and P. Walden⁷

¹*Departamento de FAMN, Universidad de Sevilla, Apartado 1065, E-41080 Seville, Spain*

²*Centro Nacional de Aceleradores, Universidad de Sevilla/Junta de Andalucía/CSIC, E-41092 Seville, Spain*

³*Instituto de Estructura de la Materia-CSIC, E-28006 Madrid, Spain*

⁴*Centro de Investigación en Ciencias Atómicas, Nucleares y Moleculares (CICANUM), CR-2060 San José, Costa Rica*

⁵*Istituto Nazionale di Fisica Nucleare-Laboratori Nazionali del Sud (INFN-LNS), I-95123 Catania, Italy*

⁶*Departamento de Física Aplicada, Universidad de Huelva, E-21071 Huelva, Spain*

⁷*TRIUMF, Vancouver, British Columbia V-6T2A3, Canada*

⁸*Department of Physics, University of York, YO10-5DD Heslington, York, United Kingdom*

⁹*Department of Astronomy and Physics, Saint Mary's University, Halifax B3H3C3, Canada*

¹⁰*Department of Physics and Astronomy, Aarhus University, DK-8000 Aarhus, Denmark*

¹¹*Centro de Física Nuclear da Universidade de Lisboa (CFNUL), 1649-003 Lisbon, Portugal*

¹²*Departamento de Física Aplicada, Universidad de Huelva, E-21071 Huelva, Spain*

¹³*Fundamental Physics, Chalmers University of Technology, S-41296 Göteborg, Sweden*

¹⁴*School of Physics and Astronomy, University of Edinburgh, EH9 3JZ Edinburgh, United Kingdom*

(Received 8 October 2012; revised manuscript received 22 December 2012; published 5 April 2013)

The inclusive breakup for the $^{11}\text{Li} + ^{208}\text{Pb}$ reaction at energies around the Coulomb barrier has been measured for the first time. A sizable yield of ^9Li following the ^{11}Li dissociation has been observed, even at energies well below the Coulomb barrier. Using the first-order semiclassical perturbation theory of Coulomb excitation it is shown that the breakup probability data measured at small angles can be used to extract effective breakup energy as well as the slope of $B(E1)$ distribution close to the threshold. Four-body continuum-discretized coupled-channels calculations, including both nuclear and Coulomb couplings between the target and projectile to all orders, reproduce the measured inclusive breakup cross sections and support the presence of a dipole resonance in the ^{11}Li continuum at low excitation energy.

DOI: [10.1103/PhysRevLett.110.142701](https://doi.org/10.1103/PhysRevLett.110.142701)

PACS numbers: 25.70.-z, 24.50.+g, 25.60.-t

Nuclear haloes are intriguing quantum phenomena associated with one or two weakly bound nucleons, which generate a dilute density distribution extending much further than the radius expected for a stable nucleus of the same mass. Breakup reactions have provided useful information on the ground state properties of halo nuclei, such as binding energies, spectroscopic factors and angular momentum (see Ref. [1] for a recent review). When exclusive measurements are possible, i.e., all outgoing fragments are detected after breakup, these experiments can be used to infer spectroscopic properties of the continuum, such as the location and spin assignment of resonant states [2–4] and dipole strengths [2,5,6]. These experiments have revealed that halo nuclei exhibit a strong soft electric dipole ($E1$) response at low excitation energies [2,6], in contrast with the case of stable nuclei, for which the $E1$ response is mostly due to the giant dipole resonance, which appears at significantly higher energies.

The largest soft dipole response ever observed corresponds to the ^{11}Li nucleus. This is a paradigmatic two-neutron halo nucleus, with a well-developed three-body structure, comprising a ^9Li core surrounded by two loosely bound neutrons [$S_{2n} = 369.15(65)$ keV [7]]. Although

reported values of the $B(E1)$ of ^{11}Li deduced from exclusive breakup measurements give a large $E1$ strength just above the breakup threshold, they considerably differ in the absolute values [1,6,8,9]. Structure models differ also in the predictions of the continuum; it is debated whether there is a low energy dipole resonance [10–14] and, if so, how important this resonance is for the appearance of the large $B(E1)$ strength.

Information on the $B(E1)$ response can be also inferred from inclusive breakup reactions, in which only the heavy fragments are detected. When the halo nucleus interacts with a heavy target, the strong dipole Coulomb interaction between them produces a drastic reduction of the elastic scattering cross section and a large breakup probability. At Coulomb-barrier energies, where the Coulomb force dominates, this process populates selectively states with low excitation energies. Therefore, a comparison between the data with suitable reaction calculations can provide an indirect determination of the $B(E1)$ at low-excitation energies.

With this motivation, we have measured the elastic scattering and breakup reaction of the ^{11}Li nucleus on a lead target at energies around the Coulomb barrier.

A detailed analysis of the elastic scattering data has been recently presented in Ref. [15]. Here, we present the breakup data and the corresponding theoretical analysis in terms of semiclassical and coupled-channels calculations. From this comparison, we have extracted information about the $B(E1)$ distribution close to the breakup threshold. The presence and location of a low-lying dipole resonance in the ^{11}Li nucleus is also investigated.

The experiment was performed at the TRIUMF facility (Vancouver, Canada). A primary 500 MeV 100 μA proton beam produced at the TRIUMF cyclotron impinged on a Ta primary target. The post accelerated Li secondary beams were transported to the ISAC-II facility [16] and monitored by a 700 μm surface barrier Si detector placed at about 28 cm from the target. The average intensity of the ^{11}Li beam detected in this monitor was 4300 $^{11}\text{Li}/\text{s}$. For ^9Li , two targets were used (1.45 and 1.9 mg/cm^2), whereas for ^{11}Li only the thinner one was used. The angular resolution was better than 3° . The measurements were done at two beam energies, 24.3 and 29.8 MeV, which are, respectively, below and around the Coulomb barrier ($V_b \approx 28$ MeV).

The experimental setup is composed by 4 telescopes ($T1$ – $T4$) placed around the ^{208}Pb target, covering the following laboratory angles: $T1$: 10° – 40° , $T2$: 30° – 60° , $T3$: 50° – 100° , $T4$: 90° – 140° . Telescopes $T1$ and $T2$ consisted of a 40 μm thick double sided Si strip detector (DSSSD) in front stacked with 500 μm DSSSDs, forming a ΔE - E pixel based structure. Telescopes $T3$ and $T4$ consisted of 20 μm single sided Si strip detectors (SSSSD) in front stacked with 60 μm DSSSDs, in order to form a ΔE - E pixel based structure.

Elastic and breakup events were selected in two-dimensional ΔE versus $\Delta E + E$ plots, as shown in Fig. 1 for the telescope 1, at a nominal angle of $30.0^\circ \pm 1.5^\circ$ and for an incident energy of 24.3 MeV. The ^{11}Li breakup events, producing ^9Li fragments, are clearly separated from the ^{11}Li elastic events, which allows a precise analysis of the ^{11}Li breakup process on ^{208}Pb . From this plot, it is seen that the average energy of the ^9Li fragments is about 1 MeV higher than $9/11$ of the incident energy of ^{11}Li , that would be the expected energy in a distant breakup scenario.

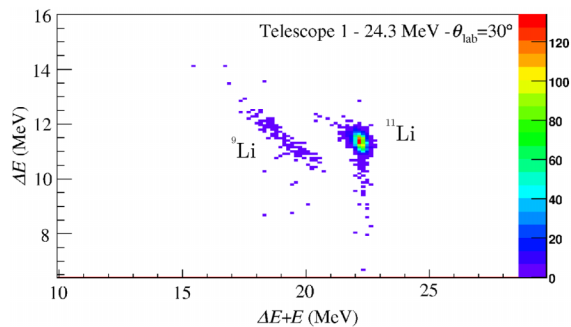


FIG. 1 (color online). ΔE versus $\Delta E + E$ plot for the telescope 1 at the laboratory angle $30.0^\circ \pm 1.5^\circ$ for the $^{11}\text{Li} + ^{208}\text{Pb}$ reaction at an incident energy of 24.3 MeV.

The observed values suggest instead a scenario in which the projectile breaks up in the proximity of the target, and then the ^9Li is postaccelerated with an energy gain equal to the potential energy at this point. For example, for a Coulomb trajectory corresponding to a scattering angle of 30° , this yields an energy gain of the order of 1–1.5 MeV, in agreement with Fig. 1.

To quantify the importance of the breakup channel, we use the breakup probability, defined here as the ratio of ^9Li events to the sum of ^9Li and ^{11}Li events for a given scattering angle. This magnitude is shown in Fig. 2, at the two incident energies. The errors indicated are purely statistical. In both cases, the breakup probability increases smoothly with increasing angle. We note that the large yield of ^9Li at backward angles is comparable to that of ^{11}Li at 24.3 MeV and 70% larger at 29.8 MeV.

The experimental breakup probabilities have been compared with continuum-discretized coupled-channels (CDCC) calculations [17], using the four-body version of this method proposed in Ref. [18]. This is an extension of the standard CDCC method appropriate for three-body projectiles. In these calculations, the ^{11}Li states (bound and unbound) are described within a three-body model ($^9\text{Li} + n + n$). To reduce the complexity of the calculations, the spin of the ^9Li core is ignored. For the n - ^9Li and n - n interactions we adopt the model P4 of Ref. [19]. An

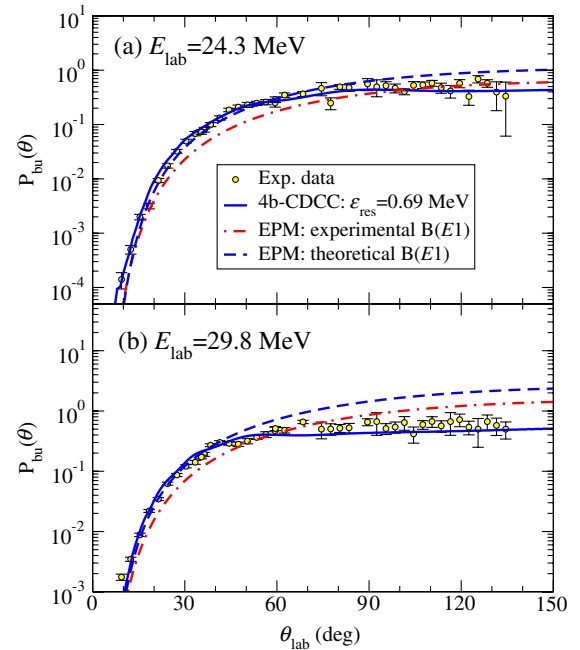


FIG. 2 (color online). Breakup probabilities angular distributions, in the laboratory frame, for the reaction $^{11}\text{Li} + ^{208}\text{Pb}$ at (a) 24.3 MeV and (b) 29.8 MeV. The circles represent the experimental data. The solid line represent the four-body CDCC calculation. The dashed and dot-dashed lines are semiclassical (EPM) calculations computed, respectively from the theoretical three-body $B(E1)$ distribution and from the experimental $B(E1)$ distribution of Ref. [6].

effective three-body force is also included to reproduce the experimental two-neutron separation energy. This gives a ground state wave function with a root mean square (rms) radius of 3.28 fm, assuming a rms of 2.44 fm for the ${}^9\text{Li}$ core [20]. Continuum states with $J_{nn}^\pi = 0^+, 1^-, 2^+$ and 3^- were included, and grouped into energy intervals, up to a maximum energy of 5 MeV, following the average *binning* method [17]. As found in other theoretical models [12–14], this three-body model predicts the existence of a low-lying dipole resonance at low excitation energies, but its position depends critically on the choice of the three-body effective interaction. Thus, for the 1^- states the strength of the three-body potential is adjusted in order to reproduce in the best possible way the breakup cross section obtained in this experiment. This gives a resonance energy of $\varepsilon_x \approx 0.69$ MeV (i.e., 0.32 MeV above the breakup threshold). This value is consistent with the prediction of Ref. [13]. The breakup probability corresponding to this calculation is shown in Fig. 2 (solid line). Note that the calculation refers to the scattering angle of the c.m. of ${}^{11}\text{Li}$ fragments, though we have checked that the effect of taking this angle instead of the experimentally determined ${}^9\text{Li}$ scattering angle is negligible, mainly for scattering angles below 50° . This calculation reproduces the data for the whole angular range and at the two measured energies. The corresponding $B(E1)$ distribution is shown in Fig. 3 (solid line). It is found to be very large in the vicinity of the threshold, being even larger than the experimental distribution obtained from the latest exclusive experiment [6], also shown in this figure by circles.

Although our four-body CDCC calculations include ${}^{11}\text{Li}$ continuum states with total angular momentum up to $J_{nn}^\pi = 3^-$ and projectile-target couplings with multipoles up to $\lambda = 3$, we have verified that, for small scattering

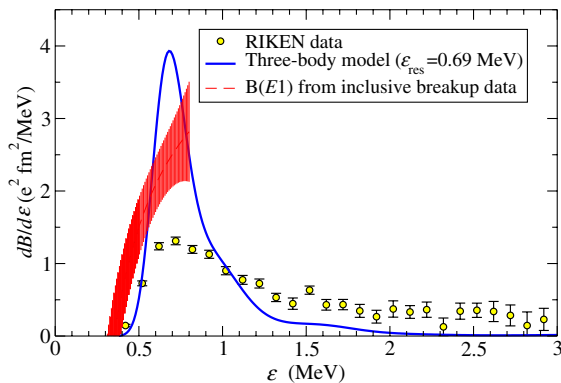


FIG. 3 (color online). $B(E1)$ distributions of ${}^{11}\text{Li}$ as a function of the excitation energy. The circles represent the experimental data from Ref. [6]. The solid line corresponds to a three-body model calculation of ${}^{11}\text{Li}$, assuming the existence of a dipole resonance at $\varepsilon = 0.69$ MeV above the ground state (0.32 MeV above the breakup threshold). The shaded region is the $B(E1)$ distribution obtained from our breakup data, using the linear approximation (5). See text for details.

angles, the breakup is due mainly to the dipole Coulomb couplings. This fact, along with the large value of the Sommerfeld parameter at these collision energies, suggests that these probabilities can be also described by the first-order semiclassical Coulomb excitation theory [21]. This is the so-called equivalent photon method (EPM). For a pure dipole excitation, the breakup probability in this model is given by

$$P_{\text{bu}}(\theta) = \left(\frac{Z_t e}{a_o \hbar v}\right)^2 \frac{2\pi}{9} \int_{\varepsilon_b}^{\infty} d\varepsilon \frac{dB(E1, \varepsilon)}{d\varepsilon} (I_{11}^2 + I_{1-1}^2), \quad (1)$$

where $I_{1\pm 1}(\theta, \varepsilon)$ are the Coulomb integrals [21]. The only structure input required by these calculations is the $B(E1)$ distribution. In Fig. 2 we present the calculations obtained with Eq. (1), using two different prescriptions for the $B(E1)$. The dashed line is the EPM calculation based on the theoretical $B(E1)$ distribution corresponding to the three-body model used in the four-body CDCC calculations (solid line in Fig. 3). This calculation agrees very well with the full CDCC calculation for scattering angles up to $\theta_{\text{lab}} \approx 60^\circ$ ($\theta_{\text{lab}} \approx 50^\circ$) for $E_{\text{lab}} = 24.3$ MeV (29.8 MeV). This agreement confirms the validity of the first-order semiclassical approximation and the dominance of the $E1$ couplings at forward angles. The second EPM calculation shown in Fig. 2 (dot-dashed line) uses the experimental $B(E1)$ distribution inferred from the exclusive breakup experiment at RIKEN [6]. This calculation follows the correct trend of the data, but underestimates its magnitude at small angles, where we expect the EPM model to be valid. Note that, if the experimental distributions of Refs. [8,9] were used, the underestimation would be even larger, since these distributions give a smaller $B(E1)$ close to the threshold. Consequently, the analysis of the present inclusive data suggests that, close to the breakup threshold, the $B(E1)$ strength in ${}^{11}\text{Li}$ could be even larger than the experimental strength reported in Ref. [6].

It is worth noting that, unlike the experimental breakup probability, the theoretical breakup probability given by Eq. (1) can be larger than unity. This is because this formula corresponds to a first-order calculation, and unitarity is not guaranteed. In fact, it can be seen in Fig. 2 that the EPM calculation for $E_{\text{lab}} = 29$ MeV becomes larger than unity at large scattering angles. At these angles, however, this model is not reliable since it neglects nuclear couplings and higher order effects.

In general, the breakup probability depends on the intrinsic properties of the projectile nucleus (${}^{11}\text{Li}$ in our case) as well as on the characteristics of the reaction (target, energy of the collision, scattering angle, nuclear and Coulomb forces). Thus, disentangling structure information, such as the $B(E1)$ distribution, from the measured cross section is a difficult task. In the following, we present a novel procedure which permits the extraction of valuable

information of the $B(E1)$ in a model-independent way. For this purpose, we consider the small angle limit of the Coulomb integrals appearing in Eq. (1),

$$I_{11}^2 + I_{1-1}^2 \approx \frac{8\pi a_0}{\hbar v} \sin(\theta/2) \varepsilon \exp(-t\varepsilon), \quad (2)$$

where t is a parameter with dimensions of the inverse of energy given by the expression

$$t = \frac{a_0}{\hbar v} \left(\pi + \frac{2}{\sin(\theta/2)} \right). \quad (3)$$

This parameter has the meaning of the collision time of the Coulomb trajectory for each scattering angle θ divided by \hbar . Inserting (2) into (1), one can collect the target charge dependence, as well as the angular and energy dependence, to define a *reduced breakup probability*, given by

$$\begin{aligned} P_r(t) &= P_{\text{bu}}(\theta) \frac{9t^2(\hbar v)^3 a_0}{16\pi^2 (Z_t e)^2 \sin(\theta/2)} \\ &= \int d\varepsilon \frac{dB(E1, \varepsilon)}{d\varepsilon} \varepsilon e^{(-t\varepsilon)t^2}, \end{aligned} \quad (4)$$

that is completely determined by the $B(E1)$ distribution, and is independent of all the collision parameters. Thus, we find that the reduced breakup probability for Coulomb-dominated breakup of halo nuclei, when plotted as a function of the collision time, obey a scaling property that is independent of the target and the projectile velocity.

In Fig. 4 we present the reduced breakup probability, in semilogarithmic scale, as a function of the collision time, for the two sets of experimental data. It is noticeable that, for both energies, the experimental points fall nicely on the same straight line, for collision times larger than 5 MeV^{-1}

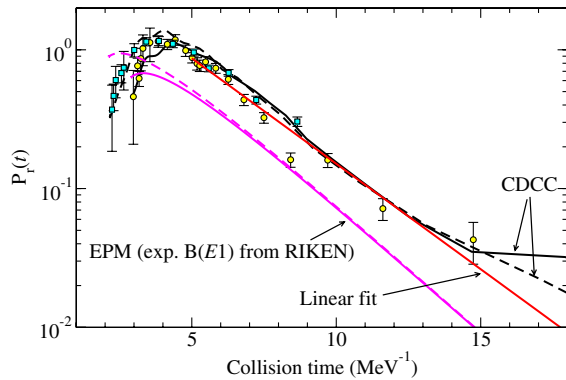


FIG. 4 (color online). Reduced breakup probability as a function of the collision time. The circles and squares correspond to the experimental data at 24.3 and 29.8 MeV, respectively. The curves are the reduced probabilities deduced from the EPM and CDCC reaction calculations presented in this work, as indicated by the labels. In each model, the solid and dashed lines correspond to the calculations at 24.3 and 29.8 MeV, respectively. The red solid line is the linear fit for $t > 5 \text{ MeV}^{-1}$, as explained in the text. For $t < 5 \text{ MeV}^{-1}$ some experimental points have been omitted for clarity.

(corresponding to laboratory angles 38° and 24° at $E_{\text{lab}} = 24.3$ and 29.8 MeV , respectively). This scaling property can be used to extract direct experimental information on the $B(E1)$ distribution from the data. For that, we note that, for large collision times, the reduced breakup probability is determined by the continuum states closer to the breakup threshold. In this region, we can approximate the $B(E1)$ distribution by a linear function, determined by an effective breakup energy ε_b , and a slope parameter b , i.e.,

$$\varepsilon \frac{dB(E1, \varepsilon)}{d\varepsilon} \approx b(\varepsilon - \varepsilon_b). \quad (5)$$

This permits us to compute analytically the integral appearing in Eq. (4), leading to the simple result

$$P_r(t) \approx b e^{-t\varepsilon_b}. \quad (6)$$

Thus, the effective breakup energy (ε_b) is determined by the logarithmic derivative of the reduced breakup probability versus the collision time, while the parameter b , associated with the slope of the $B(E1)$ distribution, is given by the values of the reduced breakup probability, extrapolated to $t = 0$.

To apply this formula to the present case, we perform a linear fit to the experimental data shown in Fig. 4, considering only the region corresponding to $t > 5 \text{ MeV}^{-1}$, where the scaling property is fulfilled. This fit, plotted by the red solid line in Fig. 4, gives $\varepsilon_b = 0.35 \pm 0.04 \text{ MeV}$ and $b = 5.0 \pm 0.3 \text{ e}^2 \text{ fm}^2/\text{MeV}$, and the corresponding $B(E1)$ distribution, parametrized according to Eq. (5), is shown in Fig. 3. The distribution is plotted only for $\varepsilon \leq 0.8 \text{ MeV}$ since, for higher excitation energies, the breakup probability, Eq. (4), is almost insensitive to the $B(E1)$ due to the exponential factor. Consequently, this procedure does not permit the extraction of the full functional form of the $B(E1)$ distribution, but it provides its behaviour for energies close to the threshold. The shaded region is the estimated error (1σ), considering that the uncertainties in the $B(E1)$ distribution increase exponentially with excitation energy. One can see that this distribution, as well as the theoretical three-body calculation, overestimate the experimental results of Ref. [6]. It is remarkable that the value of ε_b obtained by this procedure agrees very well, within the error bar, with the accepted value for the measured separation energy of ^{11}Li [7]. This encouraging result suggests a novel and powerful technique to determine separation energies of exotic nuclei from the inclusive breakup cross sections, in situations in which the direct measurement of this quantity is not feasible.

Indeed, the conditions under which the scaling property is derived are very stringent. One has to assume the semiclassical approximation, and consider only Coulomb dipole interaction to first order. We have assessed the validity of the scaling property using breakup cross sections computed from the four-body CDCC calculations. The corresponding reduced breakup probabilities, shown in Fig. 4 by

black lines, indicate that the scaling property is also fulfilled by the calculations for $t > 5 \text{ MeV}^{-1}$. The semiclassical calculations, as expected, satisfy accurately the scaling property.

We stress the fact that this novel methodology could be used to obtain the binding energy of other weakly bound nuclei whenever the angular dependence of inclusive breakup can be obtained. The fact that this method only requires the determination of the inclusive breakup cross section, makes it suitable for very exotic nuclei, for which coincidence experiments of neutrons and the charged core are not feasible.

This work has been partially supported by Spanish national projects FPA2009-08848, FPA2009-07387, FPA2010-22131-C02-01, and FPA2009-07653, and by the Consolider Ingenio 2010 Program CPAN (CSD2007-00042).

-
- [1] T. Nakamura and Y. Kondo, in *Clusters in Nuclei, Vol. 2*, Lecture Notes in Physics Vol. 848, edited by C. Beck (Springer, Berlin, 2012), pp. 67–119.
 - [2] T. Aumann *et al.*, *Phys. Rev. C* **59**, 1252 (1999).
 - [3] N. Fukuda *et al.*, *Phys. Rev. C* **70**, 054606 (2004).
 - [4] Y. Satou *et al.*, *Phys. Lett. B* **660**, 320 (2008).
 - [5] T. Nakamura *et al.*, *Phys. Lett. B* **331**, 296 (1994).

- [6] T. Nakamura *et al.*, *Phys. Rev. Lett.* **96**, 252502 (2006).
- [7] M. Smith *et al.*, *Phys. Rev. Lett.* **101**, 202501 (2008).
- [8] S. Shimoura *et al.*, *Phys. Lett. B* **348**, 29 (1995).
- [9] M. Zinser *et al.*, *Nucl. Phys.* **A619**, 151 (1997).
- [10] A. Cobis, D. V. Fedorov, and A. S. Jensen, *Phys. Rev. C* **58**, 1403 (1998).
- [11] I. J. Thompson, B. V. Danilin, V. D. Efros, M. V. Zhukov, J. S. Vaagen, and The Russian-Nordic-British Theory Collaboration, *J. Phys. G* **24**, 1505 (1998).
- [12] K. Ikeda, *Nucl. Phys.* **A538**, 355 (1992).
- [13] E. Garrido, D. V. Fedorov, and A. S. Jensen, *Nucl. Phys.* **A708**, 207 (2002).
- [14] E. C. Pinilla, P. Descouvemont, and D. Baye, *Phys. Rev. C* **85**, 054610 (2012).
- [15] M. Cubero *et al.*, *Phys. Rev. Lett.* **109**, 262701 (2012).
- [16] G. Ball, L. Buchmann, B. Davids, R. Kanungo, C. Ruiz, and C. E. Svensson, *J. Phys. G* **38**, 024003 (2011).
- [17] N. Austern, Y. Iseri, M. Kamimura, M. Kawai, G. Rawitscher, and M. Yahiro, *Phys. Rep.* **154**, 125 (1987).
- [18] M. Rodríguez-Gallardo, J. M. Arias, J. Gómez-Camacho, A. M. Moro, I. J. Thompson, and J. A. Tostevin, *Phys. Rev. C* **80**, 051601(R) (2009).
- [19] I. J. Thompson and M. V. Zhukov, *Phys. Rev. C* **49**, 1904 (1994).
- [20] A. V. Dobrovolsky *et al.*, *Nucl. Phys.* **A766**, 1 (2006).
- [21] K. Alder and A. Winther, *Electromagnetic excitation: Theory of Coulomb Excitation with Heavy Ions* (North-Holland, Amsterdam, 1975).